

Showcasing research from Professor Tomoo Mizugaki's laboratory, Graduate School of Engineering Science, Osaka University, Japan.

Reductive amination of carboxylic acids under H_2 using a heterogeneous Pt-Mo catalyst

An aluminum oxide-supported Pt-Mo ($Pt\text{-Mo}/\gamma\text{-Al}_2\text{O}_3$) catalyst exhibits high activity for the reductive amination of carboxylic acids even under 0.1 MPa H_2 pressure. $Pt\text{-Mo}/\gamma\text{-Al}_2\text{O}_3$ is reusable and applicable to the reductive amination of biomass-derived fatty acids such as lauric acid, palmitic acid, and stearic acid to provide their corresponding fatty amines in excellent yields. The unique catalysis of Pt-Mo will make a significant contribution to establish a future sustainable process for alkylamine synthesis.

As featured in:



See Tomoo Mizugaki *et al.*,
Green Chem., 2024, **26**, 2571.



Cite this: *Green Chem.*, 2024, **26**, 2571

Received 16th June 2023,
Accepted 20th December 2023

DOI: 10.1039/d3gc02155f

rsc.li/greenchem

Reductive amination of carboxylic acids under H_2 using a heterogeneous Pt–Mo catalyst†

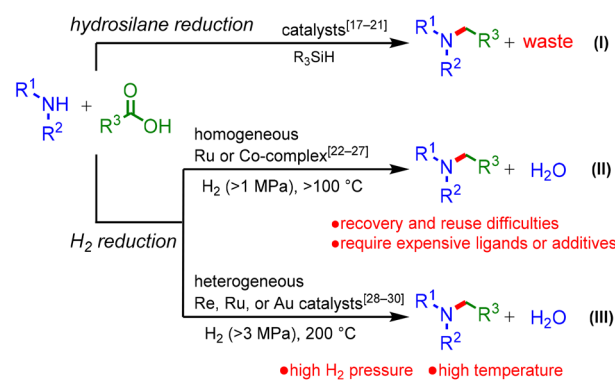
Katsumasa Sakoda,^a Sho Yamaguchi,^a Kazuki Honjo,^a Yasutaka Kitagawa,^{a,b,c,d,e} Takato Mitsudome^{a,b,f} and Tomoo Mizugaki^{a,b,c}

Reductive amination of carboxylic acids is a green and sustainable method for alkylamine synthesis because carboxylic acids are abundant and accessible carbon sources. Herein, we present an aluminum oxide-supported platinum–molybdenum (Pt – $Mo/\gamma-Al_2O_3$) catalyst that enables mild and selective reductive amination of carboxylic acids under H_2 . Pt – $Mo/\gamma-Al_2O_3$ exhibited high performance even under ambient H_2 pressure. A broad range of carboxylic acids and amines were transformed into alkylamines with good functional group tolerance. Notably, the amination of biomass-derived fatty acids led to the successful formation of the corresponding fatty amines. The catalyst was reusable at least four times without any significant loss in activity. The development of highly active heterogeneous Pt – Mo catalysts with wide applicability and reusability will significantly contribute to sustainable alkylamine production.

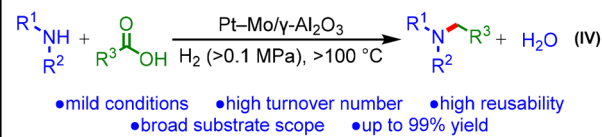
Introduction

Alkylamines are an important class of chemicals that can be used as polymers, pharmaceuticals, dyes, agrochemicals, and surfactants.¹ To date, there have been numerous reports on alkylamine syntheses based on stoichiometric or catalytic methods, including *N*-alkylation with organohalides, coupling of aryl halides with amines,^{2–4} and reductive amination of carbonyl compounds.^{5–7} Among these methods, the reductive amination of aldehydes or ketones to produce alkylamines is a reliable and widely accepted method in both research and industry. Meanwhile, carboxylic acids have been applied less frequently for reductive amination,^{8–11} despite their natural abundance and availability.^{12–14} In the previously reported reductive amination of carboxylic acids, stoichiometric amounts of $NaBH_4$ ^{15,16} or hydrosilanes^{17–21} were adopted as

reductants (Scheme 1(I)). However, these methods produce large amounts of waste. In contrast, H_2 is an ideal reductant because water is the sole co-product. Research efforts have been devoted to developing homogeneous Ru or Co catalysts for the reductive amination of carboxylic acids using H_2 (Scheme 1(II)).^{22–27} Nevertheless, these catalyst systems have serious drawbacks, including difficulty in reusing the catalyst and the requirement of expensive phosphine ligands or addi-



this work



Scheme 1 Catalytic reductive amination of carboxylic acids.



tives. To address these problems, heterogeneous catalysts have been employed because of their easy recovery and reuse; however, the reported catalyst systems require high H₂ pressures and temperatures (Scheme 1(III)).^{28–30} To attain green and sustainable reductive amination of carboxylic acids, the development of highly active heterogeneous catalysts is required.

Herein, we report the mild reductive amination of carboxylic acids with H₂ using a supported Pt–Mo catalyst (Scheme 1(IV)). This study represents the first catalyst for the reductive amination of carboxylic acids that operates under H₂ at atmospheric pressure. Furthermore, the Pt–Mo catalyst exhibits a wide substrate scope, including biomass-derived carboxylic acids, and demonstrates high reusability.

Results and discussion

Catalyst performance

Pt–Mo and the other catalysts were prepared using the co-impregnation method (see Table S1† for details). The obtained catalysts were evaluated for the reductive amination of acetic acid (2a) with piperidine (1a) to *N*-ethylpiperidine (3a) under 2 MPa H₂ at 100 °C for 12 h without any pre-reduction step (Table 1, see Table S2† for details). Notably, the aluminum oxide-supported platinum–molybdenum (Pt–Mo/γ-Al₂O₃) catalyst showed high activity, providing 3a in a 98% yield (entry 1). Catalysts using platinum-group metals (Rh, Pd, and Ru) and metal oxides (Re, W, and V) resulted in low yields of 3a (entries 2–7). The single-metal catalysts (Pt/γ-Al₂O₃ and Mo/γ-Al₂O₃) were ineffective in the reductive amination (entries 8 and 9). These results indicated that the co-presence of Pt and Mo is important for efficient reductive amination. The support effect

Table 1 Reductive amination of acetic acid (2a) with piperidine (1a) to *N*-ethylpiperidine (3a) over various supported metal catalysts^a

Entry	Catalyst	Conv. of 1a ^b [%]	Yield ^b [%]	
			3a	4a
1	Pt–Mo/γ-Al ₂ O ₃	>99	98	0
2	Rh–Mo/γ-Al ₂ O ₃	28	18	3
3	Pd–Mo/γ-Al ₂ O ₃	11	5	6
4	Ru–Mo/γ-Al ₂ O ₃	9	0	4
5	Pt–Re/γ-Al ₂ O ₃	36	28	3
6	Pt–W/γ-Al ₂ O ₃	13	9	3
7	Pt–V/γ-Al ₂ O ₃	11	2	4
8	Pt/γ-Al ₂ O ₃	7	2	3
9	Mo/γ-Al ₂ O ₃	13	0	5

^a Reaction conditions: catalyst (0.15 g), Pt: 8 mol% and Mo: 2 mol%, 1a (1 mmol), 2a (3 mmol), *n*-hexane (3 mL), 100 °C, H₂ (2 MPa), 12 h.

^b Conversion and yield were determined by gas chromatography–flame ionization detection (GC-FID) using an internal standard for analysis and calculated based on 1a.

of the Pt–Mo catalysts was also examined (Tables S3 and S4, Fig. S1 and S2† for details); consequently, the γ-Al₂O₃ and TiO₂-supported catalysts showed high yield and selectivity for the reductive amination. The turnover number (TON) value of Pt–Mo/TiO₂ surpassed that of Pt–Mo/γ-Al₂O₃. Then, the reusability of the Pt–Mo/γ-Al₂O₃ and Pt–Mo/TiO₂ catalyst was investigated (Fig. 1 and Table S5†). After the reaction, Pt–Mo catalyst was recovered by centrifugation and reused for the next run. The Pt–Mo/γ-Al₂O₃ maintained its activity in the 2nd run, but the yield of 3a decreased to 85% in the 6th run. In sharp contrast to Pt–Mo/γ-Al₂O₃, the 3a yield using Pt–Mo/TiO₂ significantly decreased in the 2nd run, clearly representing the superior reusability of Pt–Mo/γ-Al₂O₃ to Pt–Mo/TiO₂. Therefore, Pt–Mo/γ-Al₂O₃ catalyst was selected as the most suitable catalyst in terms of activity and durability (see Tables S6, S7, and Fig. S3† for details).

The high performance of the Pt–Mo/γ-Al₂O₃ catalyst was further demonstrated under H₂ at atmospheric pressure (Scheme 2a); the Pt–Mo/γ-Al₂O₃ catalyst promoted the amination of 2a with 1a to afford 3a in a 71% yield, outperforming previously reported catalysts that require 1–6 MPa of H₂.^{22–30} To the best of our knowledge, the Pt–Mo/γ-Al₂O₃ catalyst is the first example of a catalyst that can promote the reductive amination of carboxylic acid using H₂ at atmospheric pressure. The

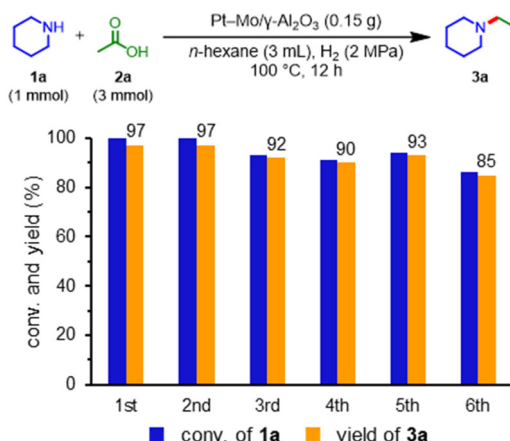
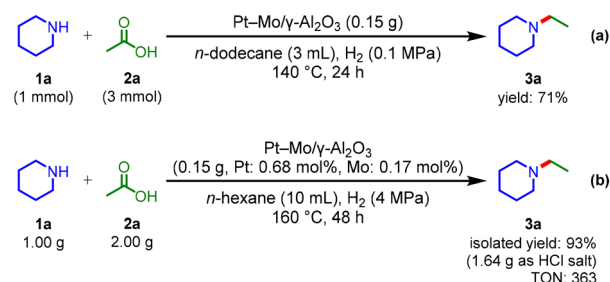


Fig. 1 Reusability of the Pt–Mo/γ-Al₂O₃ catalyst for reductive amination.

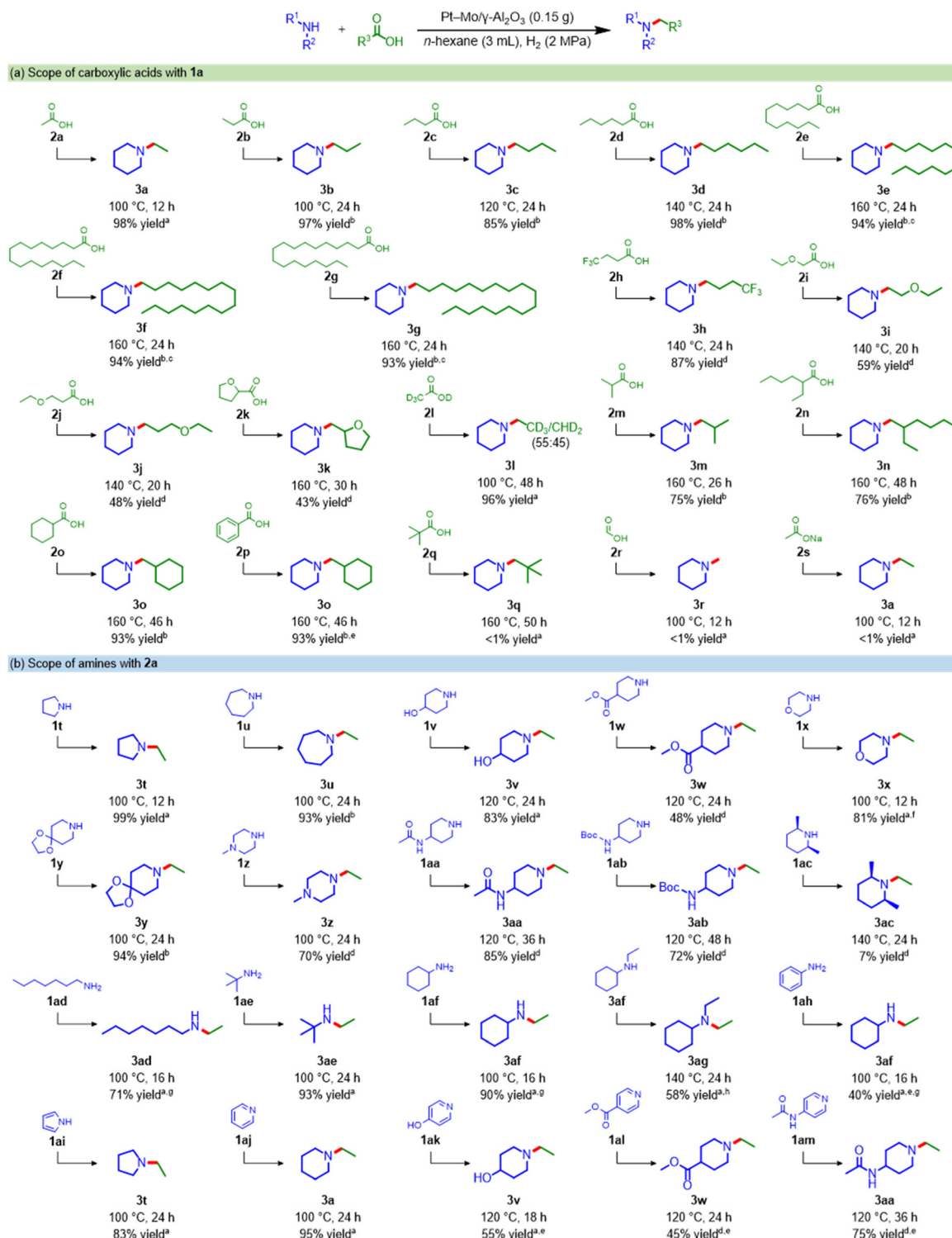


Scheme 2 (a) Pt–Mo/γ-Al₂O₃ catalyzed reductive amination under H₂ at atmospheric pressure. (b) Preparative-scale reductive amination.



Pt–Mo/γ-Al₂O₃ catalyst was also applicable to gram-scale amination (Scheme 2b); **1a** (1 g) and **2a** (2 g) were stirred at 160 °C for 48 h, and **3a** was obtained in a 93% isolated yield with a

high TON of 363 for the reductive amination of carboxylic acids (Table S8†). Overall, Pt–Mo/γ-Al₂O₃ showed high activity and good reusability in reductive amination.



Scheme 3 Reductive amination of various carboxylic acids with amines under H₂. Reaction conditions: Pt–Mo/γ-Al₂O₃ (0.15 g, Pt: 8 mol% and Mo: 2 mol%), amine (**1** mmol), carboxylic acid (3 mmol), *n*-hexane (3 mL), H₂ (2 MPa). ^a GC-FID yield. ^b Isolated yield as a hydrochloride salt. ^c Carboxylic acid (1.5 mmol). ^d ¹H NMR yield. ^e H₂ (3 MPa). ^f H₂ (4 MPa). ^g Carboxylic acid (4 mmol). ^h Carboxylic acid (5 mmol).



Substrate scope

Using the Pt–Mo/γ-Al₂O₃ catalyst, the reductive amination of various carboxylic acids with **1a** was investigated (see Scheme 3a and Table S9† for the products distribution). Notably, the Pt–Mo/γ-Al₂O₃ catalyst was applicable to naturally abundant carboxylic acids (**2a**–**2g** and **2k**). Short-chain fatty acids obtained from the waste stream, such as **2a**, propionic acid (**2b**), and butyric acid (**2c**),³¹ were successfully converted to **3a**, *N*-propyl (**3b**), and *N*-butyl piperidine (**3c**) in 98%, 97%, and 85% yields, respectively. Triglyceride-derived medium- and long-chain fatty acids such as caproic acid (**2d**), lauric acid (**2e**), palmitic acid (**2f**), and stearic acid (**2g**) reacted well with **1a** to generate the corresponding alkylamines in over 93% yield. Carboxylic acids bearing trifluoromethyl (**2h**), ether (**2i** and **2j**), and heterocycles (**2k**) were aminated in good-to-moderate yields, but slight cleavage of the C–O bond occurred. The amination of acetic acid-*d*₄ (**2l**) afforded *N*-ethyl piperidine with H–D scrambling. The Pt–Mo/γ-Al₂O₃ catalyst converted relatively bulky carboxylic acids (**2m** and **2n**) to produce the corresponding amines at a high reaction temperature (160 °C). Furthermore, leptoclaine (**3o**), which has been reported to be a respiratory stimulant,³² was obtained from cyclohexanecarboxylic acid (**2o**). **3o** was also directly produced from readily available benzoic acid (**2p**), along with the hydrogenation of the aromatic ring. The tertiary carboxylic acid (**2q**), with high steric hindrance around the acyl carbonyl carbon, was unfavorable for this catalytic system, and formic acid (**2r**) and sodium acetate (**2s**) were hardly aminated.

Next, we applied the Pt–Mo/γ-Al₂O₃ catalyst to the reductive amination of **2a** using a wide range of amines (Scheme 3b and Table S10†). The Pt–Mo/γ-Al₂O₃ catalyst exhibited high activity toward various cyclic amines, aliphatic amines, and pyridine derivatives, producing the corresponding alkylamines in high yields. Secondary cyclic amines with different ring sizes (**1a**, **1t**, and **1u**) were smoothly alkylated to afford *N*-ethyl amines in excellent yields. Importantly, various functional groups, including hydroxyl (**1v**), ester (**1w**), ether (**1x**), acetal (**1y**), amino (**1z**), amide (**1aa**), and carbamate (**1ab**), were tolerated. However, the reaction using a bulky amine, *cis*-2,6-dimethylpiperidine (**1ac**), resulted in only 7% yield. The Pt–Mo/γ-Al₂O₃ catalyst was also applicable to amination with primary amines; heptyl (**1ad**), *tert*-butyl (**1ae**), and cyclohexyl amines (**1af**) were efficiently transformed into the corresponding secondary amines. **3af** was further alkylated to produce *N,N*-diethyl cyclohexylamine (**3ag**) in 58% yield. Amination with aniline (**1ah**) gave **3af** in a 40% yield. Heteroaromatics are also potential substrates for synthesizing alicyclic amines; pyrrole (**1ai**) and pyridine derivatives (**1aj**–**1am**) were hydrogenated and converted to their corresponding tertiary alicyclic amines. These results clearly demonstrate the broad applicability of this Pt–Mo/γ-Al₂O₃ catalyst for the synthesis of a variety of alkylamines from carboxylic acids and amines.

Characterization

To investigate the catalyst structure during the reaction, Pt–Mo/γ-Al₂O₃ was pre-reduced with H₂ under the reaction conditions and characterized (see ESI† for details). Transmission

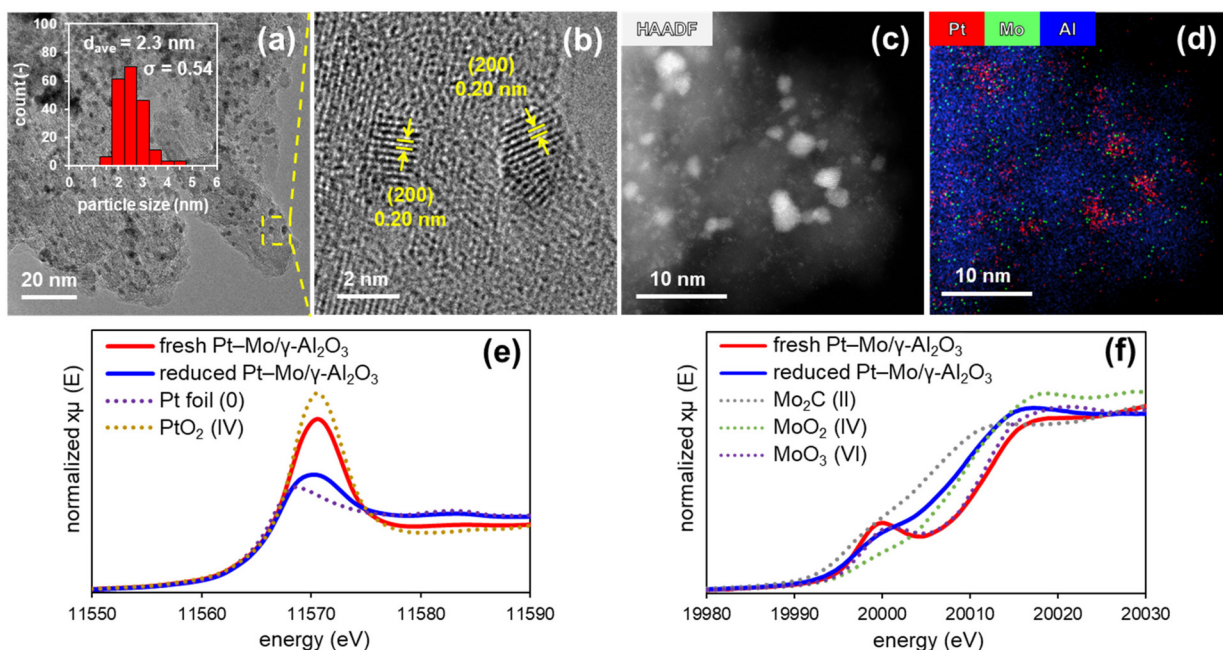


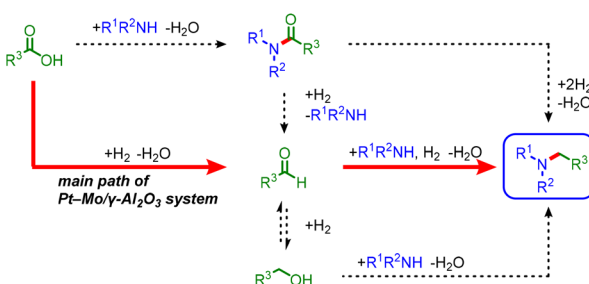
Fig. 2 (a) TEM image and size distribution histogram (inset) of reduced Pt–Mo/γ-Al₂O₃. (b) High-resolution TEM image of reduced Pt–Mo/γ-Al₂O₃ showing one-dimensional lattice fringes of the (200) lattice planes in Pt NPs. (c) HAADF-STEM image of reduced Pt–Mo/γ-Al₂O₃. (d) Composite overlay of the elemental mapping of Pt, Mo, and Al in reduced Pt–Mo/γ-Al₂O₃. (e) Pt L₃-edge XANES spectra of fresh Pt–Mo/γ-Al₂O₃, reduced Pt–Mo/γ-Al₂O₃, Pt foil, and PtO₂. (f) Mo K-edge XANES spectra of fresh Pt–Mo/γ-Al₂O₃, reduced Pt–Mo/γ-Al₂O₃, Mo₂C, MoO₂, and MoO₃.



electron microscopy (TEM) images of the reduced Pt–Mo/γ-Al₂O₃ revealed the presence of nanoparticles (NPs) with a mean diameter of 2.3 nm (Fig. 2a). A high-resolution TEM image of the NPs showed that the measured *d*-spacing value of the lattice fringe was approximately 0.20 nm, which corresponds to the (200) plane of face-centered cubic Pt NPs (Fig. 2b). High-angle annular dark-field scanning TEM (HAADF-STEM), coupled with energy-dispersive X-ray spectroscopy (EDX), confirmed the dispersion of Pt and Mo (Fig. 2c and d). The local structures of the Pt and Mo species in Pt–Mo/γ-Al₂O₃ were characterized by X-ray absorption fine structure (XAFS) analysis. The white lines in the Pt L₃-edge X-ray absorption near-edge structure (XANES) spectra of fresh and reduced Pt–Mo/γ-Al₂O₃ were similar to those of PtO₂ and Pt foil, respectively, indicating the *in situ* formation of metallic Pt species (Fig. 2e). In the Mo K-edge XANES spectra, the absorption edge energy of reduced Pt–Mo/γ-Al₂O₃ shifted toward a lower energy relative to that of fresh Pt–Mo/γ-Al₂O₃, indicating the partial reduction of Mo⁶⁺ (Fig. 2f and S4†). Overall, Pt(0) and partially reduced Mo-oxide species (MoO_x) were generated on the γ-Al₂O₃ surface under reductive amination conditions.

Reaction pathway

In the reductive amination of carboxylic acids, three possible pathways can occur *via* amide, aldehyde, or alcohol intermediates (Scheme 4).^{22–29} As shown in Scheme 3b, amide and hydroxyl groups (**3aa** and **3v**) are tolerated, suggesting that amides or alcohols are unlikely to be the major reaction intermediates. Indeed, the hydrogenation of *N*-propionylpiperidine (**4b**) in the presence of **2b** or the amination of 1-propanol with **1a** resulted in low yields of **3b** (Scheme S1a and b†). In contrast, the reductive amination of propionaldehyde with **1a** afforded **3b** in a 70% yield, indicating that the aldehyde is the major intermediate (Scheme S1c and Fig. S5†). Based on the above results, a main reaction pathway is proposed (Scheme S2†). Pt NPs dissociate H₂ to reduce MoO₃ to MoO_x,^{33,34} and carboxylic acid is adsorbed on MoO_x³⁵ and hydrogenated to give an aldehyde intermediate.³⁶ The nucleophilic attack of the amine on the aldehyde, followed by hydrogenation of the generated hemiaminal, affords an alkyl-amine.³⁷ Partially reduced MoO_x serves as a Lewis acid site for carbonyl activation (see Fig. S6 and S7† for details).^{38–40}



Scheme 4 Possible reaction pathways for the Pt–Mo/γ-Al₂O₃-catalyzed reductive amination of carboxylic acids.

Therefore, cooperative catalysis between the Pt NPs and MoO_x successfully promotes the reductive amination of carboxylic acids under H₂.

Conclusions

We developed a highly efficient Pt–Mo/γ-Al₂O₃ catalyst for the reductive amination of carboxylic acids under H₂. This is the first catalytic system that achieves the reductive amination of carboxylic acids under ambient H₂ pressure. The Pt–Mo/γ-Al₂O₃ catalyst was applicable to preparative-scale reactions with a high TON value (363). Furthermore, Pt–Mo/γ-Al₂O₃ was easily separated from the reaction mixture and the reaction could be repeated at least five times while maintaining high activity and selectivity. A wide range of substrates, including biomass-derived fatty acids, and high functional group tolerance were demonstrated, thus offering a simple and clean methodology for the reductive amination of carboxylic acids. We propose that the high catalytic performance of the Pt–Mo/γ-Al₂O₃ catalyst originates from cooperative catalysis between Pt NPs and MoO_x, and this study makes a significant contribution to the development of future sustainable reaction processes.

Author contributions

K. S. and S. Y. designed the experiments, conducted the catalytic activity tests, and characterized the catalysts. K. H. and Y. K. performed the DFT calculations. T. Mit. discussed the experiments and results. T. Miz. directed and conceived the project. K. S. and S. Y. wrote the manuscript with input from all the authors. All the authors commented on the manuscript and approved the final version.

Conflicts of interest

There are no conflicts to declare.

Acknowledgements

This work was supported by a JSPS Research Fellowship for Young Scientists (23KJ1473), JSPS KAKENHI Grant Numbers 20H02523, 21K04776, and 22H02050, and JST PRESTO Grant Number JPMJPR21Q9. This study was partially supported by JST-CREST, Grant Number JPMJCR21L5. A portion of the experimental analysis was supported by the “Advanced Research Infrastructure for Materials and Nanotechnology in Japan (ARIM)” (JPMXP1222HK0062) of the Ministry of Education, Culture, Sports, Science and Technology (MEXT). We thank Dr Toshiaki Ina and Dr Tetsuo Honma (SPring-8) for the XAFS measurements (2021B1945, 2022B1699, 2022B0519, and 2022B0586). This work was the result of using the research equipment shared in the MEXT Project for promoting public



utilization of advanced research infrastructure (Program for supporting the construction of core facilities) (Grant Numbers JPMXS0441200022 and JPMXS0441200023).

References

- 1 S. A. Lawrence, *Amines: Synthesis, Properties and Application*, Cambridge University Press, Cambridge, 2004.
- 2 S. V. Ley and A. W. Thomas, *Angew. Chem., Int. Ed.*, 2003, **42**, 5400–5449.
- 3 P. Ruiz-Castillo and S. L. Buchwald, *Chem. Rev.*, 2016, **116**, 12564–12649.
- 4 R. Dorel, C. P. Grugel and A. M. Haydl, *Angew. Chem., Int. Ed.*, 2019, **58**, 17118–17129.
- 5 T. Irrgang and R. Kempe, *Chem. Rev.*, 2020, **120**, 9583–9674.
- 6 K. Murugesan, T. Senthamarai, V. G. Chandrashekhar, K. Natte, P. C. J. Kamer, M. Beller and M. R. V. Jagadeesh, *Chem. Soc. Rev.*, 2020, **49**, 6273–6328.
- 7 M. Sheng, S. Fujita, S. Yamaguchi, J. Yamasaki, K. Nakajima, S. Yamazoe, T. Mizugaki and T. Mitsudome, *JACS Au*, 2021, **1**, 501–507.
- 8 A. Corma, S. Iborra and A. Velty, *Chem. Rev.*, 2007, **107**, 2411–2502.
- 9 P. Foley, A. Kermanshahi-pour, E. S. Beach and J. B. Zimmerman, *Chem. Soc. Rev.*, 2012, **41**, 1499–1518.
- 10 J. R. Cabrero-Antonino, R. Adam and M. Beller, *Angew. Chem., Int. Ed.*, 2019, **58**, 12820–12838.
- 11 J. Li, C.-Y. Huang and C.-J. Li, *Angew. Chem., Int. Ed.*, 2022, **61**, e202112770.
- 12 T. Werpy and G. Petersen, *Top Value Added Chemicals from Biomass: Volume I – Results of Screening for Potential Candidates from Sugars and Synthesis Gas*, 2004, DOI: [10.2172/15008859](https://doi.org/10.2172/15008859).
- 13 J. J. Bozell and G. R. Petersen, *Green Chem.*, 2010, **12**, 539–554.
- 14 K. Tomishige, M. Yabushita, J. Cao and Y. Nakagawa, *Green Chem.*, 2022, **24**, 5652–5690.
- 15 G. W. Gribble, P. D. Lord, J. Skotnicki, S. E. Dietz, J. T. Eaton and J. L. Johnson, *J. Am. Chem. Soc.*, 1974, **96**, 7812–7814.
- 16 P. Marchini, G. Liso and A. Reho, *J. Org. Chem.*, 1975, **40**, 3453–3456.
- 17 I. Sorribes, K. Junge and M. Beller, *J. Am. Chem. Soc.*, 2014, **136**, 14314–14319.
- 18 M.-C. Fu, R. Shang, W.-M. Cheng and Y. Fu, *Angew. Chem., Int. Ed.*, 2015, **54**, 9042–9046.
- 19 K. G. Andrews, R. Faizova and R. M. Denton, *Nat. Commun.*, 2017, **8**, 15913.
- 20 E. L. Stoll, T. Tongue, K. G. Andrews, D. Valette, D. J. Hirst and R. M. Denton, *Chem. Sci.*, 2020, **11**, 9494–9500.
- 21 L. Ouyang, R. Miao, Z. Yang and R. Luo, *J. Catal.*, 2023, **418**, 283–289.
- 22 A. A. N. Magro, G. R. Eastham and D. J. Cole-Hamilton, *Chem. Commun.*, 2007, 3154–3156.
- 23 I. Sorribes, J. R. Cabrero-Antonino, C. Vicent, K. Junge and M. Beller, *J. Am. Chem. Soc.*, 2015, **137**, 13580–13587.
- 24 Y. Shi, P. C. J. Kamer, D. J. Cole-Hamilton, M. Harvie, E. F. Baxter, K. J. C. Lim and P. Pogorzelec, *Chem. Sci.*, 2017, **8**, 6911–6917.
- 25 Y. Shi, P. C. J. Kamer and D. J. Cole-Hamilton, *Green Chem.*, 2017, **19**, 5460–5466.
- 26 W. Liu, B. Sahoo, A. Spannenberg, K. Junge and M. Beller, *Angew. Chem., Int. Ed.*, 2018, **57**, 11673–11677.
- 27 B. Emayavaramban, P. Chakraborty and B. Sundararaju, *ChemSusChem*, 2019, **12**, 3089–3093.
- 28 T. Toyao, S. M. A. H. Siddiki, Y. Morita, T. Kamachi, A. S. Touchy, W. Onodera, K. Kon, S. Furukawa, H. Ariga, K. Asakura, K. Yoshizawa and K. Shimizu, *Chem. – Eur. J.*, 2017, **23**, 14848–14859.
- 29 R. Coeck and D. E. De Vos, *Green Chem.*, 2020, **22**, 5105–5114.
- 30 R. Coeck, J. Meeprasert, G. Li, T. Altantzis, S. Bals, E. A. Pidko and D. E. De Vos, *ACS Catal.*, 2021, **11**, 7672–7684.
- 31 M. Atasoy, I. Owusu-Agyeman, E. Plaza and Z. Cetecioglu, *Bioresour. Technol.*, 2018, **268**, 773–786.
- 32 J. R. Boissier, C. Dumont and R. Ratouis, *Arch. Int. Pharmacodyn. Ther.*, 1967, **167**, 273–284.
- 33 K. Murugappan, E. M. Anderson, D. Teschner, T. E. Jones, K. Skorupska and Y. Román-Leshkov, *Nat. Catal.*, 2018, **1**, 960–967.
- 34 K. Sakoda, S. Yamaguchi, T. Mitsudome and T. Mizugaki, *JACS Au*, 2022, **2**, 665–672.
- 35 C. Kaku, S. Suganuma, K. Nakajima, E. Tsuji and N. Katada, *ChemCatChem*, 2022, **14**, e202200399.
- 36 L. A. Gomez, R. Bababrik, M. R. Komarneni, J. Marlowe, T. Salavati-fard, A. D. D'Amico, B. Wang, P. Christopher and S. P. Crossley, *ACS Catal.*, 2022, **12**, 6313–6324.
- 37 Y. Nakamura, K. Kon, A. S. Touchy, K. Shimizu and W. Ueda, *ChemCatChem*, 2015, **7**, 921–924.
- 38 A. S. Touchy, S. M. A. H. Siddiki, K. Kon and K. Shimizu, *ACS Catal.*, 2014, **4**, 3045–3050.
- 39 T. Mizugaki, Y. Nagatsu, K. Togo, Z. Maeno, T. Mitsudome, K. Jitsukawa and K. Kaneda, *Green Chem.*, 2015, **17**, 5136–5139.
- 40 M. Shetty, E. M. Anderson, W. H. Green and Y. Román-Leshkov, *J. Catal.*, 2019, **376**, 248–257.

